Pressure tuning of the motional behavior of Li^+, Ag^+, and Cu^+ ions in shallow off-center potentials of alkali halides

Ulrich Holland* and Fritz Lüty
Physics Department, University of Utah, Salt Lake City, Utah 84112
(Received 19 June 1978)

The delicate balance of interaction energies, which creates in certain alkali halides a shallow off-center potential for small substitutional defect ions, can be drastically altered by application of relatively small (<7 kbar) hydrostatic pressure (corresponding to about 1% lattice compression). This has been investigated for KCl:Li^+, NaBr:Cu^+, RbCl:Ag^+, and RbBr:Ag^+ by measurements of the real and imaginary dielectric response of the off-center dipoles, and by absorption-strength measurements of the Ag^+ and Cu^+ forbidden $d \rightarrow s$ uv transitions (which become partially allowed in the odd-parity off-center potential). Applied pressure reduces gradually the central and rotational barriers of the multiwell potential and, while keeping the off-center dipole moment constant, drastically increase the dipolar reorientation rates. As a consequence, the observable range of relaxation frequencies (10^2–10^5 Hz) shifts under pressure to low temperatures, tuning through regimes of thermally activated motion with decreasing barriers into regimes of tunneling motion. Similar to the situation in the superionic conductors, a particular match between cavity and point-ion size produces an optimum "local ionic mobility" at lowest temperatures. Slightly higher lattice compression leads to the disappearance of this ionic mobility, due to a change of the defect potential into a centrosymmetric one. This off- to on-center transition (a "localized analog" to pressure-induced displacive phase transitions in ferroelectrics) is discussed in terms of its first- or second-order character. The question of whether pressure induced changes in the phonon dressing ("polaron effect") of the dipoles can contribute to the observed relaxation changes will be discussed, too.

I. INTRODUCTION

Spontaneous changes of symmetry properties in a crystalline solid can occur both as collective effect of the total lattice, or as a localized effect at a point defect. In a cubic $BaTiO_3$ crystal, for instance, the Ba^{2+} and Ti^{4+} sublattice can become *collectively displaced* relative to the O^{2-} sublattice, producing a *perment electric dipole* and a low-symmetry *ferroelectric crystal structure.*[1] A localized analog to this can occur for certain point-ion defects in cubic alkali-halide lattice. A small point ion, substituted into a relatively large cavity, can move out of the cavity center, because it gains energy mainly by polarization interaction until it is balanced by short-range repulsion interaction. This delicate energy balance creates an *off-center potential*, which in a cubic crystal will have equivalent energy minima in either the six ⟨100⟩, the eight ⟨111⟩, or the 12 equivalent ⟨110⟩ directions. The resulting off-center displacement of the defect ion will produce a *localized permanent electric dipole* at the defect site,[2] which is accompanied by gerade distortions (of E_g and/or T_{2g}) symmetry and therefore also has *elastic dipole* character.[3]

A transition between the cubic and collectively displaced state of a ferroelectric crystal can be induced by changes of the pressure or temperature of the system.[4] As illustrated in Fig. 1, hydrostatic pressure P can change the effective potential in such a way that the sublattice displacement disappears either gradually towards zero under $P \rightarrow P_c$ (*second-order phase transition*), or disappears abruptly at $P = P_c$ (*first-order phase transition*).

Small point-ion defects (like Li^+, Ag^+, Cu^+, F^-) have been observed in various alkali-halide hosts to be either in the centrosymmetric or the off-

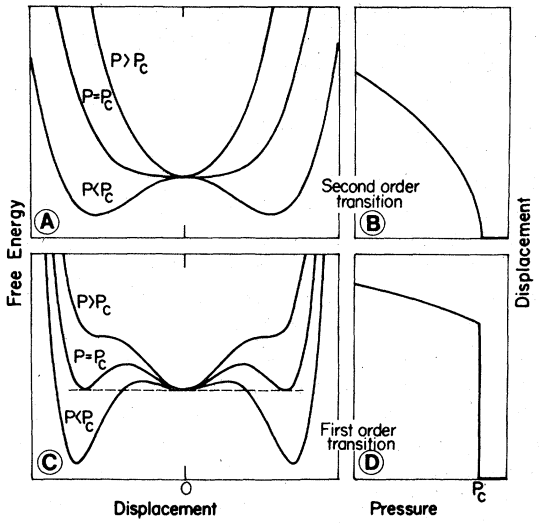

FIG. 1. Schematic pressure variation of the free energy vs displacement and of the resulting displacement (at the energy minimum), for second- and first-order transitions.

center state. Temperature-induced transitions between these two states can hardly be measured, because the presence of an off-center state (with its weak $1/T$ paraelectric and paraelastic properties) can be detected basically only at low temperatures. Hydrostatic pressure, on the other hand, applied to a shallow off-center defect system at low temperature, should increase the repulsion interaction and thus drastically offset the delicate energy balance producing the off-center potential. Theoretical calculations with microscopic interaction models[5] have not always been successful in predicting the existence and symmetry of an off-center state for a certain defect system. These calculations, however, definitely showed the crucial dependence of the resulting potential on the chosen Born-Mayer parameters.[6] We therefore address ourselves in this work to the question of whether hydrostatic pressure can induce (first- or second-order-type) *transitions between off-center and centrosymmetric states of a defect*,[7] similar to the displaced ferroelectric case in Fig. 1.

The second main question of interest in this work is the effect of pressure (equals lattice-parameter change) on the *motional behavior* of the point defect in the off-center multiwell potential. As opposed to the more or less fixed orientation of the collective displacement in a ferroelectric domain or single crystal, the small localized electric and elastic dipole of the off-center defect can easily reorient among the equivalent orientational states. Depending on the strength and shape of the potential and on the ion mass, this reorientation can—in different temperature ranges—be based either on quantum-mechanical tunneling or classical thermally activated motion over a barrier. In the tunneling motion, the lattice distortions of T_{1u}, E_g, and T_{2g} symmetry connected with the off-center defect, play a decisive role, hindering the dipole motion by strong dressing or "polaron" effects.[8] Under field or stress applications, i.e., for reorientation among slightly *unequal* potential wells, the tunneling process must be accompanied by the absorption or emission of phonons—involving either single- or multiphonon processes ("phonon-assisted tunneling").[9]

Tuning of the off-center potential strength (and maybe the defect-lattice interaction) by hydrostatic pressure, should drastically affect all the above-mentioned possible reorientation processes. These processes can be detected and differentiated by different temperature dependences of the dipole-lattice relaxation rates. Measurements of the dipole relaxation behavior over a wide temperature range under hydrostatic pressure should therefore allow one to study the motion of point ions in a well-characterized tunable model potential. This can supply important insights, parallels, and model cases for the general field of ionic motion in solids—in particular superionic conductors.

Optical and dielectric techniques will be used to monitor the static and dynamic dipole properties under hydrostatic pressure for various off-center defects (Ag^+, Cu^+, and Li^+) in various alkali-halide hosts. After a short description of the experimental techniques (Sec. II), we present and discuss the optic (Sec. III) and dielectric results (Sec. IV) and give a comprehensive discussion in Sec. V.

II. EXPERIMENTAL TECHNIQUES

Optic and dielectric measurements were performed under hydrostatic pressure (using helium gas as pressure medium) at temperatures between $T = 300$ K and $T = 1.5$ K. The pressurizing system of a standard design included a mobile cart in which the pressure was intensified from a 2-kbar tank. This cart carried also the cryostat (top-loading gas-flow-cooled type) in an adjustable mount, facilitating access to the different measurement systems.[10] Two pressure cells for optical and dielectric measurements were constructed of heat-treated maragin steel.

The pressure was monitored measuring the resistance of a manganin gauge with a Mueller bridge (in steps down to 10^{-4} Ω). The achieved accuracy (±1 bar relative, $\pm\frac{1}{2}\%$ absolute) holds down to the freezing curve of helium.[11] Below this curve, possible clogging effects at the entrace fitting and thermal contraction of the solid helium give rise to higher uncertainties of the pressure value. The temperature was measured with a silicon-diode sensor on top of the pressure cells. The temperature of the sample in the cell is estimated to be within 1 K, when the pressure cell is cooled, and cooler by less than 0.5 K when the cell is heated up (for $T > 4$K). For $T < 4$K, the difference is estimated to be 0.2 and 0.1 K, respectively.

The crystals were grown with the Kyropoulus technique by the University of Utah Crystal Growth Laboratory from ultrapure material, doped with 10^{-2}–10^{-4} mol parts Cu^+, Ag^+, and Li^+ salts in the melt. The resulting defect concentrations in the crystal ranged from 10^{-3}–10^{-5}. For the dielectric measurements, a special technique described in Ref. 12, was applied to produce very thin crystals with high capacitance, which at the same time were mechanically stable.

The property changes in alkali halides reported here appear at pressures of several kilobars, which correspond to lattice-parameter reductions of about $\frac{1}{2}\%$. Since low-temperature compressibility data are not available, the lattice-param-

eter changes are derived from elastic-constant data at liquid-helium temperature[13] and from room-temperature data of the slightly pressure-dependent compressibility.[14]

III. uv ABSORPTION

A. Lattice potentials and absorption strength

The lowest excitations of free Ag^+ and Cu^+ ions are parity-forbidden transitions $(n\text{-}1)d^{10} \rightarrow (n\text{-}1)d^9ns$ ($n=4$ for Cu^+ and $n=5$ for Ag^+). When the metal ions are brought as substitutional defects into a cubic crystal, these transitions become partially allowed by odd-parity distortions leading to uv absorptions of various oscillator strengths and temperature dependencies. The ungerade distortions, which destroy the inversion symmetry of the defect and mix d^9p states into the even-parity states, can be of two types: (i) Odd-parity lattice or resonance modes produce, by dynamic mixing of electronic states, an oscillator strength, which at low temperatures (due to zero-point motions) will be about $f \approx 10^{-3}$ Å^2 and will increase with temperature. (ii) Off-center displacement of a defect ion, accompanied by ungerade distortions of the surrounding lattice, produce, by *static* mixing of electronic states, a rather large oscillator strength, $f \approx 10^{-2}$–10^{-1} Å^2.

Measurements of the absorption strength of the Ag^+ and Cu^+ uv transitions in various hosts as a function of temperature therefore allow conclusions on the centrosymmetric or off-center potential of these defects. From the extended experimental and theoretical work on this subject, mainly by the group in Frankfurt,[15] the following four basically different cases be derived (see Fig. 2): (*a*) *harmonic on-center potential*: Coupling to a single harmonic oscillator mode ω will provide $f \propto \coth(\hbar\omega/kT)$ (e.g., NaCl:Ag^+); (b) *anharmonic on-center potential*: Coupling to anharmonic vibrations will provide $f \propto \sqrt{T}$ for higher T (e.g., NaCl:Cu^+); (c) *shallow off-center potential*: with small central barrier U_f. $f \propto 10^{-2}$ at $T=0$, decreasing $f \propto -T$ until off-center pocket states are "thermally filled" at $T \approx U_f$ (U_f in temperature units). For $T > U_f$: $f \propto \sqrt{T}$ like in case (ii) (e.g., RbCl:Ag^+); (d) *deep off-center potential* with large energy barrier $U_f \gg T$. $f \approx$ const (e.g., KCl:Cu^+). To illustrate the essential physical approach to this problem (and for later comparison with experiment), we summarize briefly a recent theoretical treatment by Nagasaka,[16] which follows similar lines as earlier theoretical work.[15] Starting with a ground state $(n\text{-}1)d^{10}$, a first excited state $(n\text{-}1)d^9ns$, and a higher-lying charge transfer state, in which an electron from a neighboring anion is transferred to a metal ion $(n\text{-}1)d^{10}ns$,

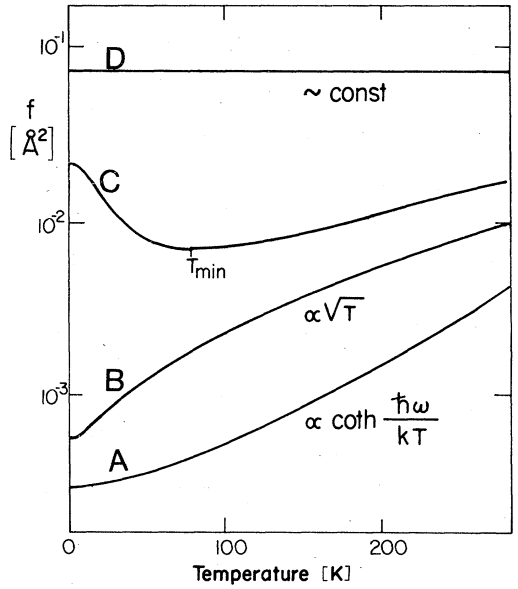

FIG. 2. Schematic temperature dependence of the oscillator strength f for different types of defect potentials: A, harmonic on-center; B, anharmonic on-center; C, shallow off-center; D, deep off-center.

Nagasaka assumes a strong mixing of the A_{1g} ground state with the T_{1u} charge-transfer state by linear electron-phonon coupling with odd modes of T_{1u} symmetry. The resulting partial electron exchange leads to stronger binding between metal and halogen ion, and eventually to a central instability of the Ag^+ and Cu^+ ion.

Similar to Glinchuk *et al.*,[17] Nagasaka choses the adiabatic potential V of the ground state by including a linear electron-phonon interacting term (due to odd-parity modes) in the Hamiltonian and by expanding the harmonic potential up to second order:

$$V(R) = \tfrac{1}{2}k^*(1-2\alpha)R^2 + (k^{*2}/2U)\alpha^2R^4. \quad (1)$$

The parameter α is defined

$$\alpha \equiv A^2/2Uk^* \quad (2)$$

with A the electron-phonon coupling constant, $2U$ the energy difference between the ground and charge transfer state, k^* the force constant, and R the normal coordinate of the vibration. This potential corresponds to the ones shown in Fig. 1(A). When $\alpha < 0.5$, the impurity ions are stable at the regular lattice site while for $\alpha > 0.5$, the regular lattice site becomes unstable, and the impurity is stabilized in an off-center position:

$$R_{\min}^2 = (1 - 1/4\alpha^2)2\alpha U/k^*. \quad (3)$$

Nagasaka derives the absorption line shape I for the transition from the ground state to the first

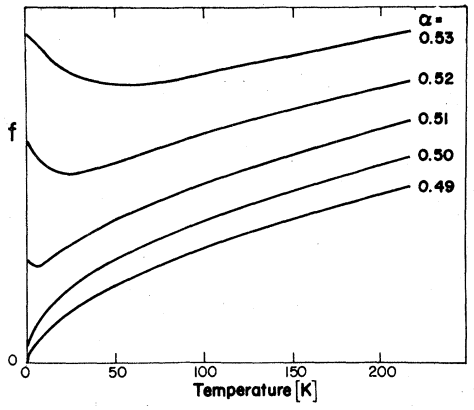

FIG. 3. Temperature dependence of the oscillator strength f for different parameters α, obtained by numerical integration, using Eq. (4) from Nagasaka (Ref. 16).

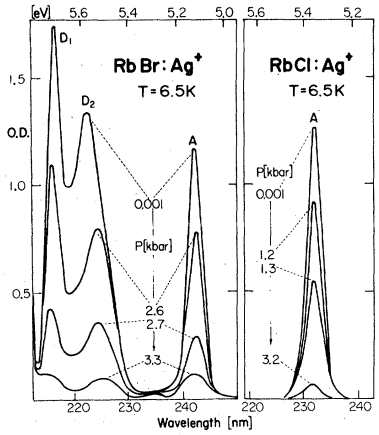

FIG. 4. Absorption spectra for Ag^+ in RbBr and RbCl, measured under different hydrostatic pressure at $T = 6.5$ K.

excited state:

$$I(X) = \frac{1}{2I_0}\left(\frac{X-U}{4\alpha U(X+U)}\right)^{1/2} \exp\left(-\frac{X^2 - 4\alpha UX - U^2}{4\alpha UkT}\right), \tag{4}$$

where $X = h\nu - h\nu_{max} + U$ and

$$I_0 = \int_0^\infty dR \exp[-V(R)/kT]\,. \tag{5}$$

From Eq. (4) the oscillator strength can be obtained by numerical integration. Figure 3 shows the calculated temperature dependence of the oscillator strength. The minimum temperature T_{min} of f when $\alpha > 0.5$ is related to the central barrier heights U_f by

$$kT_{min} = U_f = U\alpha(1 - 1/2\alpha)^2\,. \tag{6}$$

The α dependence of the off-center displacement obtained from Eq. (3) yields a similar behavior as the $R(P)$ curve in Fig. 1(B). The α dependence of the oscillator strength f, obtained from numerical integration of Eq. (4) exhibits a smooth decay of f with decreasing α.

B. Results for shallow off-center systems: RbCl:Ag^+, RbBr:Ag^+, and NaBr:Cu^+

Figure 4 shows uv spectra for Ag^+ in RbCl and RbBr at low temperature. The three absorption bands A, D_2, and D_1 correspond to optical transitions polarized parallel [110] and perpendicular ($[1\bar{1}0]$, [001]) to the [110] dipole axis.[18,19] (For RbCl:Ag^+ the D bands could not be measured because of the absorption of the sapphire windows of the pressure cell below $\lambda = 215$ nm.) The application of hydrostatic pressure leads to a strong reduction of the integrated absorption, which is similar for all three bands A, D_2, and D_1. This reduction does not occur uniformly under pressure, but is particularly pronounced between $P = 2.6$ and 2.7 kbar for RbBr:Ag^+ and $P = 1.2$ and 1.3 kbar for RbCl:Ag^+. Spectral measurements under hydrostatic pressure of the type in Fig. 4 were performed over a wide range of temperature. From their integration, the temperature dependence of the oscillator or dipole strength for various pressures were obtained, as plotted for RbCl:Ag^+ in Fig. 5. (Very similar results, obtained for RbBr:Ag^+, are not shown here[10].) For both systems, decreases of the oscillator strength under pressure are observed, which are very pronounced at low temperatures (as large as a factor

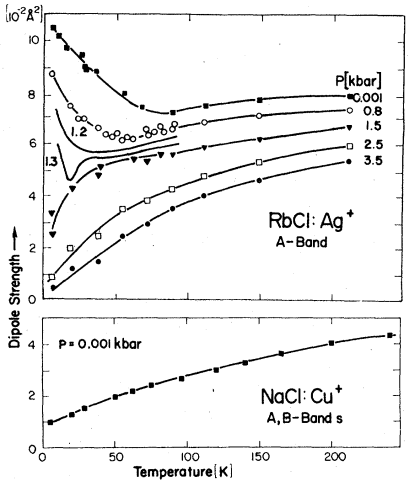

FIG. 5. Measured temperature dependence of the dipole strength for RbCl:Ag^+ under different hydrostatic pressure P and for NaCl:Cu^+ at atmospheric pressure. (In this figure, not the relative oscillator strength, but the dipole strength D is plotted, adjusted to its absolute value, reported in Ref. 15).

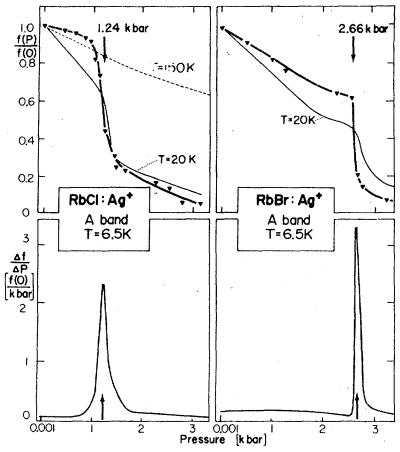

FIG. 6. Hydrostatic pressure dependence of the relative oscillator strength (upper part of the figure), and of its pressure derivative (lower part of the figure) for Ag^+ in RbCl and RbBr at $T = 6.5$ K. $f(P)$ curves at 20 and 150 K are shown, too, for comparison.

of 20) and relatively small at high temperatures.

The temperature dependence of the dipole strength of RbCl:Ag^+ at atmospheric pressure (in Fig. 5) shows a typical behavior for a shallow off-center potential [see case (c) in Fig. 2]; at several kilobars, however, the behavior of RbCl:Ag^+ becomes comparable in size and temperature dependence to that of the NaCl:Cu^+ system at atmospheric pressure (lower part of the figure), which is known to be an anharmonic on-center system [case (b) in Fig. 2]. When comparing Fig. 5 with Fig. 3, one can see that the theory, with α parameters $\alpha = 0.53$ and 0.49, describes fairly well the RbCl:Ag^+ system for pressures $P = 0.001$ and 3.5 kbar, respectively. We can therefore conclude *that the pressure has apparently changed the shallow off-center potential of the* Ag^+ *ion into an anharmonic on-center potential* [case (c) → (b) in Fig. 2].

The transition between these two cases can occur, in principle, via a gradual (second-order type) or a more abrupt change in the potential and resulting physical properties. In the first case, the observed $f(T)_p$ curves (Fig. 5) should correspond to calculated $f(T)_\alpha$ curves (Fig. 3), with a continuous variation of α from 0.53 to 0.49. A cut of the measured $f(T)_p$ diagram at different temperatures shows at high temperatures (150 °K) indeed a smooth, almost linear, $f(P)$ variation (Fig. 6), which could be well described by the similarly smooth calculated $f(\alpha)$ variation. With decreasing temperature, however, the measured $f(P)_T$ behavior becomes increasingly nonuniform, leading at low temperatures to a distinct jump in a very small pressure range (Fig. 6). This behavior is

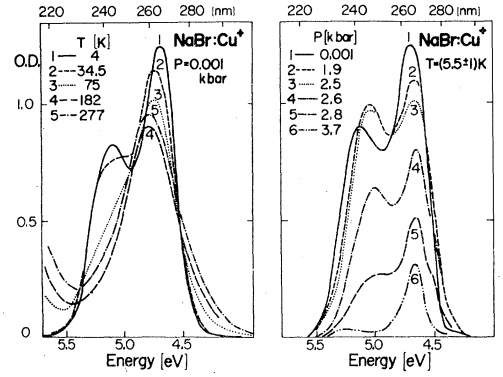

FIG. 7. Absorption spectra (optical density vs energy) for NaBr: Cu^+. Left-hand side: measured at atmospheric pressure for different temperatures; right-hand side: at $T = 5.5$ K for different hydrostatic pressures P.

in marked contrast to the calculated $f(\alpha)$ variation, which is expected to be smooth at low temperatures, too. Evidently, the measured $f(T)_p$ curves, in the intermediate pressure range, can *not* be described over the whole temperature range by a set of calculated $f(T)_\alpha$ curves (with $0.53 > \alpha > 0.49$), or in other words: the transition from shallow off-center to anharmonic on-center potential can *not* be accounted for, within the given theoretical model, by a gradual α tuning of the potential.

The NaBr:Cu^+ system has been investigated in this work for the first time with optical-absorption techniques.[7] It displays a single uv band at room temperature (RT), which develops into a double band—with two components of similar strength—when cooled below 90 K (Fig. 10 left-hand side). Application of hydrostatic pressure reduces both these absorptions by more than a factor of 10 at $T = 5.5$K (Fig. 7 right-hand side). The temperature dependence of the oscillator strength (Fig. 8) displays a behavior very similar

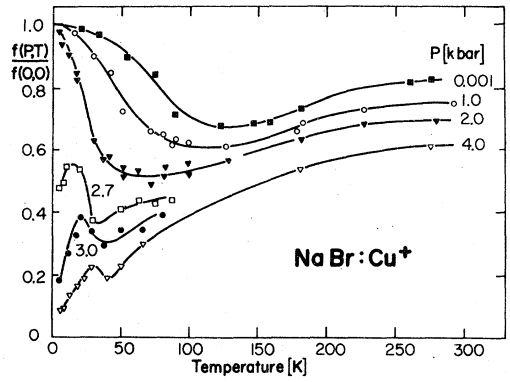

FIG. 8. Temperature dependence of the relative oscillator strength for NaBr:Cu^+ under hydrostatic pressure P.

to the one obtained for RbCl:Ag^+ and RbBr:Ag^+. This indicates that NaBr:Cu^+ is a shallow off-center system, which can be tuned by hydrostatic pressure into an anharmonic on-center situation. Again, the transition between these two end points occurs, at low temperatures, extremely nonuniform in pressure, as can be seen in Fig. 8. A low-temperature cut of this diagram shows that the integrated total absorption (of both bands) is completely pressure independent up to over 2 kbar, and then decreases abruptly around 2.7 kbar. The explicit $f(P)$ dependence will be displayed later in comparison to dielectric data (Fig. 16).

C. Deep off-center systems: KCl:Cu^+ and NaI:Cu^+

KCl:Cu^+ is known to be a deep off-center system (type D in Fig. 2) with a high ($f \simeq 10^{-1}$) and rather temperature-independent oscillator strength produced by a large off-center displacement and potential barrier $U > T$. For such a system we do not expect any sizable effect on the absorption strength from the modest pressures applied here. We found indeed that possible oscillator strength decreases were smaller than 3%/kbar in the whole temperature range and up to 6 kbar. Similar results were obtained for NaI:Cu^+ (a system not investigated previously), indicating that it is a deep off-center case too.

D. Anharmonic on-center system: NaCl:Cu^+

If the pressure-induced reduction of the α parameter, observed for the off-center systems, persists for the on-center defects too, an anharmonic on-center potential should be tuned by pressure towards the harmonic behavior. As an example of this case, NaCl:Cu^+ was studied over the whole temperature range under pressures of up to 4 kbar. Reductions of the oscillator strength (up to ~20%) were observed at temperatures above 80 K changing the initial $f(T) \propto \sqrt{T}$ dependence towards the behavior expected for the harmonic potential [case b → a in Fig. 2]. The final expected $\coth(\hbar\omega/kT)$ behavior, however, was not reached in this P range.

Similar results for NaCl:Cu^+ have been observed by Emura[20] down to liquid-N_2 temperature under $P = 3$ kbar. These are the *only* low-temperature uv absorption data under pressure previous to the ones reported here. At room temperature a variety of defect systems has been investigated under pressure.[21]

E. Absorption shifts under hydrostatic pressure

Besides the pronounced changes in the *strength* (zero moment) of the absorption discussed so far, the pressure induces small *shifts* (first-moment changes) in all absorption bands measured (see, e.g., Fig. 4). Most of the observed absorptions shift under pressure in the "normal" way to high energies (Table I), which corresponds to their observed "normal" temperature shifts in the same direction under cooling (equals lattice contraction). The only systems with observed negative pressure shifts, both bands in NaBr:Cu^+ (Fig. 7) and the D_2 band in RbBr:Ag^+ (Fig. 4), exhibit an abnormal inverted temperature shift as well. Our pressure shifts measured at RT (Table I and Ref. 10) are in close agreement with RT values measured previously by other authors.[20,21]

TABLE I. uv-absorption peak shifts under hydrostatic pressure.

System	Absorption band	Temperature	$\Delta E/E\Delta P$ (% $kbar^{-1}$)
RbCl:Ag^+	A	LHeT [a]	+0.2
RbCl:Ag^+	A	RT–38 K	+0.1
RbBr:Ag^+	D_1	LHeT	+0.3
RbBr:Ag^+	D_2	LHeT	−0.2
RbBr:Ag^+	A	LHeT	+0.1
NaCl:Cu^+	$\lambda = 257$ nm	27 K	+0.26
NaBr:Cu^+	$\lambda = 244$ nm	LHeT	−0.7
NaBr:Cu^+	$\lambda = 265$ nm	LHeT	~−0.2
NaI:Cu^+	$\lambda = 256$ nm	LHeT	+0.2
KCl:Cu^+	$\lambda = 259$ nm	LHeT	+0.23
KCl:Cu^+	$\lambda = 259$ nm	LN_2T [c]	+0.22
KCl:Cu^+	$\lambda = 259$ nm	RT	+0.16

[a] LHeT: liquid-helium temperature.
[b] RT: room temperature.
[c] LN_2T: liquid-nitrogen temperature.

IV. DIELECTRIC RESPONSE

Dielectric techniques can yield important information on both the *statics* (dipole moment approximately equal to the off-center displacement) and the *dynamics* (reorientation kinetics by tunneling or classical motion) of off-center defects. In this section, we first briefly introduce the underlying theoretical models and relations (Sec. IV A) before presenting and discussing the experimental data (Secs. IV B and IV C).

A. Static and dynamic dielectric constant

A dilute system of interaction-free permanent electric dipoles of moment $\langle p \rangle$ and dipolar polarizability α_D will contribute to the dielectric constant of a crystal, according to the Clausius-Mossotti relation, from which the dipolar contribution to the dielectric constant ϵ_D is derived to be:

$$\epsilon_D \equiv \epsilon_i - \epsilon_p = (\epsilon_i + 2)(\epsilon_p + 2)\,\tfrac{4}{9}\pi N \alpha_D , \qquad (7)$$

where ϵ_p and ϵ_i are the dielectric constant of the pure host (p) and the host with impurities (i). For small-field E ($\langle p\rangle E \ll kT$, always valid in this work) all dielectric properties are isotropic and all relations hold equally for dipoles of ⟨100⟩, ⟨111⟩, or ⟨110⟩ symmetry.

We differentiate the following cases.

(i) For *interaction-free classical permanent dipoles*, the Langevin-Debye equation holds,

$$\alpha_D = \langle p\rangle^2/3kT\,, \tag{8}$$

so that $\epsilon_D \propto \langle p\rangle^2/T$.

(ii) For dipoles, *tunneling between equivalent wells*, the degenerate orientational ground state of the dipoles becomes split (tunneling splitting Δ in temperature units). The polarizability, for small fields $\langle p\rangle E \ll k\Delta$, is given by[22,23]

$$\alpha_D = (2\langle p\rangle^2/3\Delta)\tanh(\Delta/2T)\,. \tag{9}$$

For $T \gg \Delta$, α_D approaches the classical $(1/T)$ dependence, while for $\Delta \ll T$ (when only the lowest tunneling level is occupied) a constant α_D results.

The above relations for α_D considered in the static limit ($\omega = 0$) of an applied field, yield the static dielectric response $\epsilon_D(0)$. Under applied ac field of frequency $\omega = 2\pi\nu$, the dipolar response can, in general, be described by a *complex dielectric constant* $\epsilon(\omega) = \epsilon'(\omega) - i\epsilon''(\omega)$. For a dipole system with a single relaxation time the Debye equations hold.[24] The dielectric loss $\tan\delta = \epsilon'':\epsilon'$ is given by the well-known Debye peak, the integration of which yields

$$\int \tan\delta(\omega)\, d(\log_{10}\omega) \approx \frac{\epsilon_D(0)}{1.47\,\epsilon_p} \propto \frac{\langle p\rangle^2}{T}. \tag{10}$$

This equation, together with Eqs. (7) and (8), allows one to derive $\langle p\rangle$ from loss data. In the frequency range of dielectric loss, the dipole polarization can no longer follow the driving field $E(\omega)$ and therefore $\epsilon_D(\omega)$ decreases with increasing ω.

The relaxation rate τ^{-1} of the dipole system will always be strongly affected by the *temperature*, with the particular (T) dependence reflecting the underlying dipole lattice coupling mechanism.[25] For classical, *thermally activated* rate processes, the relaxation rate is given by

$$\tau^{-1} = \tau_0^{-1}\exp(-U_\delta/T) \tag{11}$$

with τ_0 the attempt frequency and U_δ the activation energy in kelvin. For tunneling dipoles, dielectric relaxation (between wells slightly different in energy by field application) can occur by *phonon-assisted tunneling processes*, yielding for one-phonon processes[8]:

$$\tau^{-1} = A\Delta^2 T\,, \tag{12}$$

and for multiple-phonon assisted tunneling,

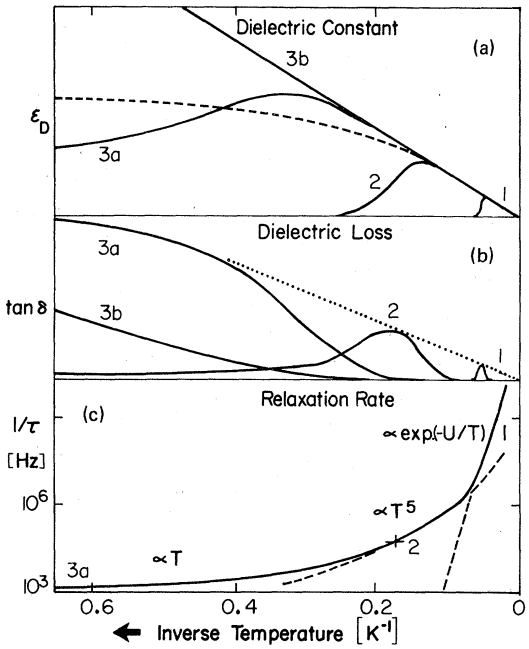

FIG. 9. Calculated dielectric response as a function of inverse temperature for the assumed relaxation rates $\tau^{-1}(T)$ in (c). Curves are shown for the chosen frequencies: (1) $\omega = 10^7$ Hz, (2) 3×10^4 Hz, (3a) 10^3 Hz, (3b) 30 Hz. The dashed curve in (a) is calculated for tunneling [Eq. (9)] with $\Delta \approx 0.3$ K.

$$\tau^{-1} = BT^\gamma \tag{13}$$

with γ expected to lie in the range $3 < \gamma < 6$.

In the presence of these three processes, the resulting temperature dependence of the relaxation will be given by the sum

$$\tau^{-1} = A\Delta^2 T + BT^\lambda + \tau_0^{-1}\exp(-U_\delta/T)\,. \tag{14}$$

With increasing temperature the predominant process will change from the left- to the right-hand-side terms in Eq. (14). As $\tau^{-1}(T)$ determines directly the loss maximum $[\omega_{\max}\tau(T) = 1]$, the Debye peak will be shifted under temperature variation over a wide frequency range. In Fig. 9(c) we illustrate—on an inverse temperature scale—an assumed (but representative!) $\tau^{-1}(T)$ behavior of the type in Eq. (14). Instead of measuring full $\delta(\omega)$ and $\epsilon(\omega)$ curves for different temperatures, it is often much more practical and economic to determine ϵ and δ at a fixed frequency as a function of T. In Figs. 9(a) and 9(b) we display the calculated $\epsilon(T)$ and $\delta(T)$ response (at different fixed frequencies), corresponding to a dipole system with the $\tau^{-1}(T)$ behavior given in Fig. 9(c). Measurements with very high frequencies in the temperature range of classical reorientation would yield a steep freezing in of ϵ and δ at rather high temperatures. Lowering of the measurement

frequency would shift the loss peak and ϵ_D drop to lower temperatures (into the range of relaxation by tunneling). For low enough measurement frequencies, finally, a loss-free $\epsilon_D \propto T^{-1}$ behavior would result. (If the tunneling splitting Δ is sizable, this $\epsilon_D \propto T^{-1}$ curve would level off for $T < \Delta$.)

For actual dielectric measurements with a normal capacity bridge, the available "frequency window" is much more limited ($\nu = \omega/2\pi = 10^2 - 10^5$ Hz), often confining $\delta(T)$ measurements to a very small temperature range. The additional (very strong!) effect of hydrostatic pressure, however, will allow in many cases to tune the various $\tau(T)$, $\epsilon(T)$, and $\delta(T)$ behavior illustrated in Fig. 9 through the narrow frequency window available for measurements.

B. Dielectric background effects from the host and data analysis

The dielectric constant ϵ_i of the doped material is always a composition of contributions from the pure host (ϵ_p) and from the dipoles (ϵ_D). For temperatures below 35 K the host-lattice part ϵ_p is essentially temperature independent. The dipolar contribution ϵ_D, on the other hand, with its $1/T$ dependence becomes measurable only below 35 K. ϵ_p can therefore be regarded as a constant background to the strongly temperature-dependent ϵ_D part and can be subtracted at $T = 35$ K (or at $T = 2$ K if the dipolar polarizability freezes in). The measured capacity at these temperatures together with the known value for ϵ_p at 2 K (from Ref. 26) allows one to determine the geometric capacity C of the sample. This is necessary in order to derive from the measured capacity data $C(P, T)$ the ϵ values $\epsilon = C/C_0$.

Under hydrostatic pressure, both dielectric constant parts ϵ_D and ϵ_p are changing. (The decrease in lattice parameter under pressure is relatively small, so that the geometric capacity C_0 can be regarded as approximately constant.) The dielectric constant decrease $d\epsilon_p/dP$ of the host material, however, is sizable; it was measured for pure NaBr and was found to be about 1.3%/kbar, independent of temperature and linear in P. It is assumed that the pressure effects on the two dielectric constant parts $\epsilon_p(P)$ and $\epsilon_D(P)$ are again additive, so that the latter can be derived from $\epsilon_i(P)$ measurements for each pressure by subtracting the ϵ_p background, as described above.

A particular background effect is present in RbBr:Ag^+, where the capacity is found, after an initial steady decrease with pressure, to rise sharply around 4 kbar at low temperatures. This effect, which is similar to the one observed previously[27] at RT, is caused by the pressure-induced lattice phase transition of RbBr from the NaCl into the CsCl structure. (As our measurements were performed only under stepwise *increasing* pressure, no hysteresis effects as seen in Ref. 27 were observed.) Together with the RT data,[27] our measurements allow for the first time to complete a P vs T phase diagram for RbBr to low temperatures, showing a considerable shift of the critical pressure to smaller values for lower temperatures.

When ϵ_D is derived from dielectric *loss* data, the evaluation is much more straight forward: As no dielectric loss background from the host exists in the low temperature regime, and ϵ_p appears only as a factor in the evaluation (Eq. 10), the dipole moment $\langle p \rangle_\delta$ derived from loss data is generally more accurate than the value $\langle p \rangle_\epsilon$ derived from dielectric constant data.

C. Experimental results

1. NaBr:Cu^+

Figure 10 shows—in a similar way as for the calculated model case in Fig. 9—a summary of typical dielectric data under pressure, plotted against inverse temperature. From the high-temperature slope of the ϵ_D curve [Eqs. (7) and (8)] and from integration of the dielectric loss [Eq. (10)], the

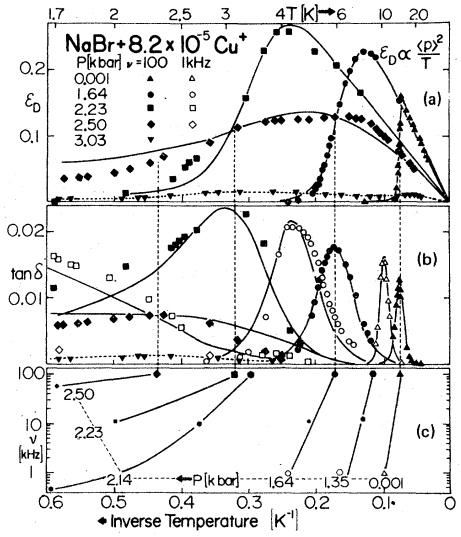

FIG. 10. Dielectric behavior of NaBr:Cu^+ under hydrostatic pressure P measured at different frequencies ν (kHz) plotted against inverse temperature. (a) Dipole contribution to the eielectric constant ϵ_D. (b) Loss tangent tanδ. (c) Frequency ν of maximum loss in a log scale. The measured behavior (points) is compared to the calculated one, using best-fit values for the dipole moment $\langle p \rangle$ and the relaxation rates $\tau^{-1}(T)$ determined in (c).

dipole moment $\langle p\rangle$ can be obtained, if the dipole concentration N is known. Together with an analysis of N (by atomic absorption spectroscopy) the dielectric constant data yield $\langle p\rangle_\epsilon = 0.54\ e$ Å [Eq. (7)] and the loss data $\langle p\rangle_\delta = 0.47\ e$ Å [Eq. (10)].

Under hydrostatic pressure, the dipole moment (as observed by ϵ and δ) does not change appreciably up to 2.23 kbar, but then decreases very strongly. At $P = 3.03$ kbar the dielectric response becomes temperature independent, indicating the total disappearance of any dipolar contribution.

In terms of the dynamic dipole response, the measurement in Fig. 10(a) shows that for $T < 14$ K at atmospheric pressure and $\nu = 100$ kHz the dipoles cannot follow the applied ac electric field anymore, freeze in and do not contribute to the dielectric constant ϵ_D. This leads to a peak in the dielectric-loss tangent at the same temperature [Fig. 10(b)]. For $\nu = 1$ kHz the maximum loss appears at a lower temperature $T = 10$ K. From measurements of this type [Fig. 10(b): $\tan\delta(T)_\nu$ or from data not shown here: $\tan\delta(\nu)_T$] the temperature dependence of the frequency of maximum loss $\nu_{max}(T) = (1/2\pi)\tau^{-1}(T)$ was obtained for each pressure case and plotted logarithmically against inverse temperature in Fig. 10(c). For atmospheric pressure an Arrhenius-type $\tau^{-1}(T)$ dependence [Eq. (11)] is obtained with an activation energy $U_\delta = 174$ K and an attempt frequency $\tau_0^{-1} = 2 \times 10^{12}\ \text{sec}^{-1}$. Under hydrostatic pressure the relaxation rate increases in the whole temperature range [Fig. 10(c)] and the "freezing in" of the dipoles (at fixed frequencies) is shifted to lower temperatures [Figs. 10(a) and 10(b)]. Up to 2.14 kbar the activation energy U_δ and attempt frequency decrease continuously under pressure (the latter one by about one decade per kilobar). At 2.14 kbar, the Arrhenius behavior, with $U_\delta = 32$ K, changes at about $T = 2.6$ K into a low-temperature ($\tau^{-1} \propto T^{4.5}$) behavior, characteristic for multiphonon-assisted tunneling. Further pressure increase produces finally a relaxation behavior $\tau^{-1} \propto T^{1.9}$ close to the $\tau^{-1} \propto T^1$ dependence expected for pure one-phonon-assisted tunneling.

With this $\tau^{-1}(T)$ behavior for each pressure determined from measuring frequencies of maximum loss, the full $\epsilon_D(T, P)$ and $\tan\delta(T, P)$ behavior could be calculated by using Eqs. (7), (8), (14) and the Debye equations, and plotted with solid lines into Figs. 10(a) and 10(b). While for the high-temperature (low-pressure) data a good fit can be obtained directly with single τ expressions, a distribution of relaxation rates had to be assumed for the high-pressure low-temperature cases, in order to account for the observed loss peaks with larger width than a Debye peak. For the last curve before the collapse of the dipolar

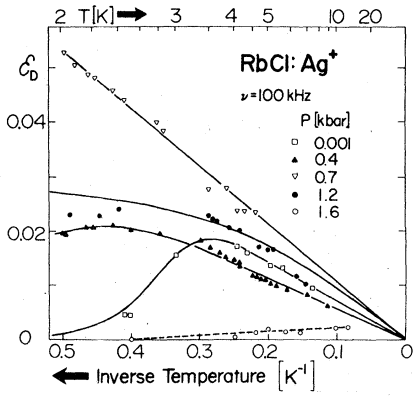

FIG. 11. Dipole contribution to the dielectric constant ϵ_D plotted against inverse temperature for RbCl:Ag$^+$ for different hydrostatic pressures P. The measured behavior (points) is compared to the calculated one with best fit values for different relaxation rates and dipole moments.

polarizability (at 2.5 kbar), no satisfactory fit could be obtained with any type of classical dipole expression. A good fit, as shown in the solid line, results, however, if a large tunneling splitting ($\Delta = 12$ K) is assumed to be present and Eq. (9) is used instead of Eq. (8).

2. *RbCl:Ag$^+$*

The pressure dependent dipole contribution to the dielectric constant for RbCl:Ag$^+$ is shown in Fig. 11. (Note the relatively small contribution, $\epsilon_D/\epsilon_i \approx 0.04/4.5 < 1\%$, which leads to a large error bar in the dipole moment $\langle p\rangle$.) The temperature at which the dipoles freeze in ($T \approx 3$ K for atmospheric pressure) is shifted under 0.4 kbar to 2 K, and for 0.7 kbar to low temperatures outside the range of the measurement. For higher pressures, ($P = 1.2$ kbar) ϵ_D deviates from a linear $(1/T)$ dependence below $T \approx 3.5$ K. As no loss is connected with this ϵ_D dispersion effect, it can only be caused by a large tunneling splitting; $\Delta = 7$ K gives a good fit with Eq. (9). For a slightly higher pressure (1.6 kbar) the dipole contribution to the dielectric constant disappears completely.

3. *RbBr:Ag$^+$*

Integrated dielectric-loss measurements on crystals of different Ag$^+$ concentrations $N = 10^{17}$–$10^{18}\ \text{cm}^{-3}$ revealed deviations from the $\epsilon_D \propto 1/T$ dependence for the higher-doped crystals. Assuming that dipole-dipole interaction causes this effect, ϵ_D/N was plotted with a Curie-Weiss law. As Fig. 12 shows in a double logarithmic plot a good fit for all concentrations can be obtained, yielding a Curie temperature of $T_c = 410 N\langle p\rangle^2/k\epsilon_p$.

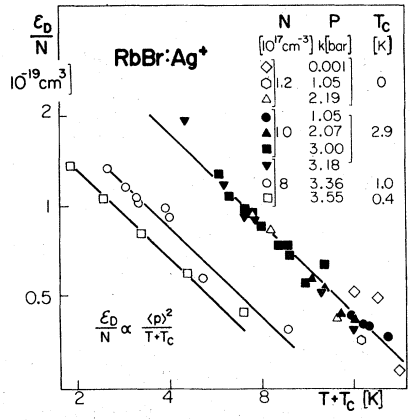

FIG. 12. RbBr:Ag^+. Log-log plot of the dielectric constant normalized to the defect concentration ϵ_D/N vs temperature under different hydrostatic pressures P. ϵ_D is derived from dielectric-loss data and plotted with a Curie-Weiss law, resulting in a Curie temperature: $T_C \approx 410N\langle p\rangle^2/k\epsilon_D$.

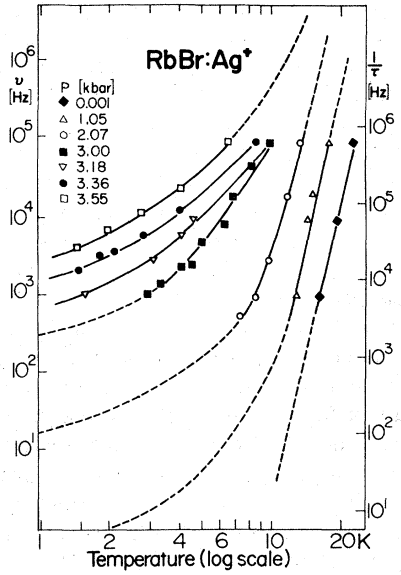

FIG. 13. Relaxation behavior of RbBr:Ag^+ under hydrostatic pressure P. Frequency of maximum loss (proportional to relaxation rate τ^{-1}) vs temperature in a log-log plot. The measured behavior (points) is compared to the calculated one with best-fit values for the different relaxation rates. An extrapolation of the $\tau^{-1}(T)$ bahavior beyond the frequency range available for measurement is indicated by dashed lines.

Under hydrostatic pressure the dipole moment is found to be constant up to $P = 3.18$ kbar and then starts to reduce to about 60% at 3.55 kbar (Fig. 12). The pressure-induced reduction of the dipole moment leads to a decrease in dipole-dipole interaction, i.e., to a corresponding reduction in the Curie temperature in agreement with the above expression for T_C. Measurements at higher pressures are not possible because RbBr undergoes a lattice phase transformation from NaCl to CsCl structure at $P \approx 3.7$ kbar for $T = 4$ K (see Sec. IV B).

The dynamic dielectric behavior of Ag^+ in RbBr was extensively studied by either $\tan\delta(T)_\omega$ or $\tan\delta(\omega)_T$ measurements which show strong shifts of τ with temperature and hydrostatic pressure. Beyond the NaCl→CsCl structural phase transition ($P = 3.55$ kbar), the loss peak does not shift any more but becomes much broader in frequency and reduced in area.

From measurements of the type in Fig. 10 and from $\tan\delta(T)_\omega$ curves, the relaxation behavior $\tau^{-1}(T)$ was obtained under different pressures (Fig. 13). Similar to NaBr:Cu^+, the relaxation rate for RbBr:Ag^+ shows a reduction of the activation energy under pressure up to $P = 2$ kbar, with no change in the attempt frequency observed within experimental error. Above $P = 3$ kbar the $\tau^{-1}(T)$ behavior derived from the measurements indicates multiphonon ($\propto T^5$) and finally one-phonon-assisted tunneling ($\propto T$) processes.

In order to better illustrate the nature of the pressure-induced relaxation changes, we have extrapolated the $\tau^{-1}(T)_p$ curves in Fig. 13 beyond the frequency range available for measurements. This should make it clear that the pressure possibly does *not* change the temperature ranges in which the different types of relaxation occur. Instead, the pressure increases the relaxation rates in *all* these three regimes, with the effect of *tuning different parts of the overall relaxation behavior at different temperatures into our limited frequency window of observation.*

In both the RbBr:Ag^+ and NaBr:Cu^+ cases, it was observed that the loss peaks for high pressure and low temperature become appreciably wider than single τ Debye peaks. This can have two reasons: (i) Towards lower temperature, dipole-dipole interaction effects increase and lead to a distribution of relaxation times. (ii) Inhomogeneity of the hydrostatic pressure causes a smearing out of relaxation times. Assuming that only effect (ii) causes the loss broadening, the size of the pressure inhomogeneity can be estimated. As the pressure shift of the relaxation time $\tau(P)$ is well determined from our experiments, the observed loss broadening can be easily translated into the pressure inhomogeneity, which would cause the corresponding τ distribution. The derived half-width of the hydrostatic pressure distribution dP/P is found to be smaller than 8% [and must be regarded as an upper limit due to the total neglect of process (i)].

For NaI:Cu^+ no dipole contribution to the dielectric constant was found down to liquid-helium temperature at atmospheric pressure. Even though

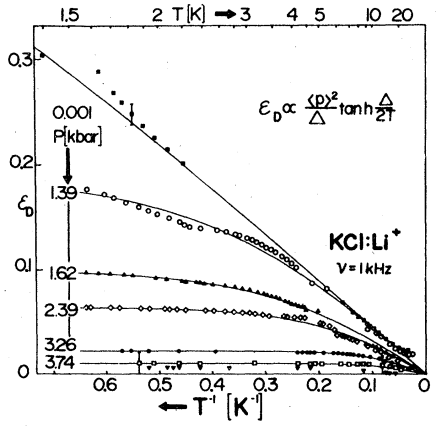

FIG. 14. Dipole contribution to the dielectric constant ϵ_D of KCl:^{7}Li$^+$ for different hydrostatic pressure P plotted against inverse temperature. The measured behavior (points) is compared to the calculated one with best fit values for the dipole moment $\langle p\rangle$ and tunneling splitting as given in Fig. 15. The highest pressure (▼) is 4.57 kbar.

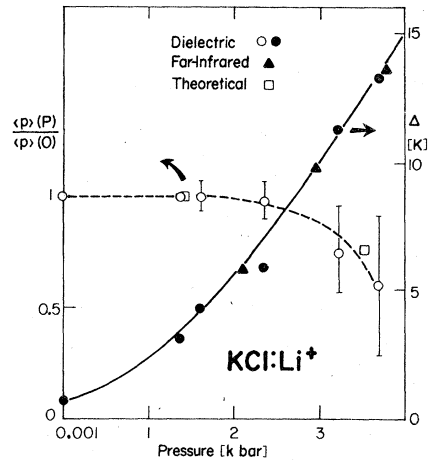

FIG. 15. Best-fit values for the dipole moment $\langle p\rangle$ and the tunneling splitting Δ of KCl:^{7}Li$^+$ as a function of hydrostatic pressure. Dielectric values for Δ are compared to the far-infrared ones (full curve, right-hand scale, see Ref. 30). $\langle p\rangle$ values from dielectric measurements are compared to the calculated off-center displacement (dashed curve, left-hand scale, see Ref. 6).

the temperature dependence of the uv absorption strength indicates a deep off-center potential for Cu$^+$ in NaI, the orientational motion of the off-center Cu$^+$ ion might be frozen in already at temperatures higher than $T = 30$ K, similar to Cu$^+$ in the potassium halides.[28,29] Electro-optic or ionic-thermocurrent (ITC) measurements would be needed to test whether Cu$^+$ is off center in NaI. In summary, the Cu$^+$ ion in the sodium halides is found either in an anharmonic on-center (NaCl), in a shallow off-center (NaBr), or in a deep off-center potential (NaI).

In KCl:Li$^+$, the defects are known to tunnel between the eight different ⟨111⟩ off-center orientations, their ground state being split by a sizable tunneling energy ($\Delta = 1.2$ K for ^{7}Li$^+$). The dipole contribution to the dielectric constant for this case, $\epsilon_D \propto (\langle p\rangle^2/\Delta)\tanh(\Delta/2T)$, [Eq. (10)], has been measured as a function of the applied pressure (Fig. 14). For high temperatures ($\Delta \ll T$) ϵ_D approaches the classical Langevin-Debye expression $\epsilon_D \propto \langle p\rangle^2/T$ (the slope and hence the dipole moment are decreasing with pressure), while for low temperatures ($\Delta \gg T$) ϵ_D levels out at $\epsilon_D \propto \langle p\rangle^2/\Delta$. The "bending over" occurs at $T \approx (\frac{3}{4})\Delta$. For atmospheric pressure ($\Delta = 1.2$ K) this bending happens at temperatures below the lowest ones measured here, while at $P = 1.39$ kbar, it can be detected and yields $\Delta = 4$ K. The tunneling splitting is increasing with increasing pressure, yielding for the highest pressure ($P = 3.74$ kbar) a value of $\Delta = 15$ K.

Best-fit values for $\langle p\rangle$ and Δ under pressure are shown in Fig. 15. Our dielectric results for $\Delta(P)$ are in good agreement with far-infrared results under pressure by Kahan *et al.*[30] The observed decrease of $\langle p\rangle$ under pressure cannot be followed accurately beyond 3.8 kbar, because the dipole contribution $\epsilon_D \propto \langle p\rangle^2/\Delta$ with $\Delta > 15$ K becomes smaller than the uncertainties from the background separation $\epsilon_i - \epsilon_\beta$. Calculated values for the off-center displacement from Quigley and Das[6] are included in Fig. 15 for comparison.

V. DISCUSSION

A. Pressure tuning of dipole reorientation (for $P < P_c$)

Our optical and dielectric experiments under hydrostatic pressure show that small changes of the lattice parameter ($-da/a \simeq 10^{-3}$–10^{-2}) have profound effects on shallow off-center defect systems. In order to interpret these effects, we first summarize the properties and quantities, which characterize the multiwell potential and the motional properties of the point defect, showing their relation to measured quantities:

(a) The detected dipole moment $\langle p\rangle$ can be directly taken as a measure for the *off-center displacement* $|R|$ of the single-charged defect ion. This dielectrically determined $\langle p\rangle$ (based on the validity of the Lorentz-field correction) is related to the uncorrected dipole moment $\langle p\rangle_u$ (as determined, e.g., in electro-optical experiments[19]) by $\langle p\rangle = 3\langle p\rangle_u/(\epsilon_\beta + 2)$.

(b) The electric dipole symmetry (as determined by electro-optical[19] or paraelectric reso-

nance[31] experiments) yields the *symmetry* ($\vec{R}$) *and multiplicity of the off-center defect states.*

(c) The *strength* of the multiwell potential is determined by the height of various energy barriers, separating the off-center pocket states: (i) The *central barrier height* U_f appears in the case of parity-forbidden optical transitions as the temperature of minimum oscillator strength f [Eq. (6)]. (ii) As the dipoles reorient by rotation rather than inversion [see (d) below], the activation energy in dielectric relaxation ($\tan\delta$) experiments yields the *reorientation barrier* U_δ, separating the dipole states along the path of predominant reorientation [Eq. (11)].

(d) The *angle of predominant reorientation* θ_R can be determined by electro-optical[19] and dielectric measurements under stress.[32]

(e) The noncubic gerade distortions (elastic dipole tensor β) of E_g and/or T_{2g} symmetry, are obtained from the splitting of the dipole states under stress of $\langle 100\rangle$ (E_g) or $\langle 111\rangle$ (T_{2g}) symmetry.

(f) The *low-lying excitations* of the defects can be classified into (i) tunneling splitting Δ (observed by paraelectric resonance[31] or by dielectric measurements[23]) [Eq. (12)], (ii) resonance modes ω_{res} of the defect, measurable by far-infrared or Raman experiments.[33]

These quantities, as far as they are known from this and other works, are summarized in Table II for the four defect systems of principal interest here. Under hydrostatic pressure, all of these quantities can, in principle, change, though only part of these changes are observable in our experiments:

(i) The pressure dependence of $|R|$ is observed directly by the dielectrically measured $\langle p\rangle$ (P), and indirectly by the measured uv oscillator strength $f(P)$. In Fig. 16 we summarize these results for the Cu^+ and Ag^+ defects, while $\langle p\rangle$ (P) for Li^+ in KCl is shown in Fig. 15.

(ii) The pressure-induced change of the optically determined central barrier U_f and the dielectrically determined reorientation barrier U_δ is summarized in Fig. 17. Figure 17 includes the calculated pressure dependence of U_f and $U_\delta = 34$ K at atmospheric pressure for Li^+ in KCl.[6]

(iii) In KCl:Li^+, the pressure tuning of all low-lying excitations was measured by Kahan *et al.*[30] with far-infrared spectroscopy; the obtained $\Delta(P)$ variation is in full agreement with our dielectric data (Fig. 15).

The observed pressure dependencies for the four systems lead to a consistent picture for the behavior in the $P < P_c$ range. In agreement with expectations from model calculations, small lattice compressions (<1%) lead to a gradual lowering of the potential barrier of the multiwell potential. This pressure tuning affects the central barrier U_f and rotational barrier U_δ in a rather parallel way, and has similar magnitudes dU/dP for all systems (Fig. 17). Consistent with this picture it was observed,[10] that the preexponential factor (attempt frequency ν_0) decreases steadily under pressure (e.g., in NaBr:Cu^+ from 10^{12} to 10^{10} sec^{-1} for $P = 0 \rightarrow 2.1$ kbar). The off-center displacement $|R|$ of the ion, as measured by the electric dipole moment, however, remains essentially constant under pressure for $P < P_c$ (Fig. 16).

TABLE II. Quantities determining the static and dynamic off-center behavior of four-defect systems.

	KCl:$^7Li^+$	NaBr:Cu^+	RbCl:Ag^+	RbBr:Ag^+
$\lvert R\rvert$ (Å)	0.51 [b]	0.5 [a]	0.36 [c]	0.44 [c]
$\vec{R}$	$\langle 111\rangle$ [b]	?	$\langle 110\rangle$ [c]	$\langle 110\rangle$ [c]
U_f (K)	139 [d]	128 [a]	82 [a]	94 [a]
U_δ (K)	35 [d]	174 [a]	34 [f]	255 [a]
$\beta(E_g)$ (10^{-23} cm^3)	0	?	0.83 [e]	1.46 [e]
$\beta(T_{2g})$ (10^{-23} cm^3)	0.4	?	0.19 [e]	0.39 [e]
θ_R	70°	?	90° [c]	90° [c]
Δ (K)	1.2 [b]	?	<0.01 [f]	?
ω (K)	61 [g]	?	31, 38, 53 [g]	?

[a] This work.
[b] Reference 31.
[c] Reference 19.
[d] Reference 6.
[e] Reference 18.
[f] Reference 34.
[g] Reference 33.

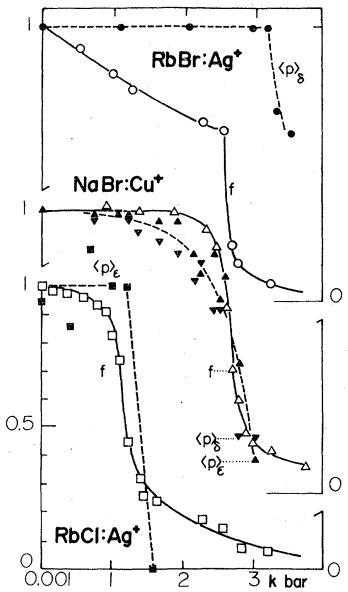

FIG. 16. Summary of the experimental manifestations of pressure-induced-off- to on-center transitions at low temperatures: optical oscillator strength (f) and electric dipole moment $\langle p\rangle$ (determined from dielectric constant $\langle p\rangle_\varepsilon$ and loss data $\langle p\rangle_\delta$), in RbBr:Ag$^+$, NaBr:Cu$^+$, and RbCl:Ag$^+$, as a function of pressure.

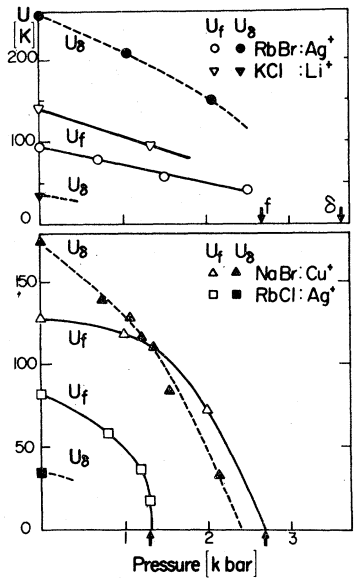

FIG. 17. Hydrostatic pressure dependence of the central barrier U_f and rotational barrier U_δ, as measured in this work for NaBr:Cu$^+$, RbCl:Ag$^+$, and RbBr:Ag$^+$, and as calculated for KCl:Li$^+$ by Quigley and Das (Ref. 6). The arrows at the abscissa indicate the observed P_c values for the off- to on-center transition. [For RbBr:Ag$^+$, two different P_c values are observed in optic (f) and dielectric (δ) measurements.]

These observations make it very unlikely that the symmetry of the dipole states $\vec{R}$, the reorientation angle θ_R, and the elastic dipole components $\beta(E_g)$ and $\beta(T_{2g})$ change under pressure.

Within this picture of a multiwell potential of constant symmetry and off-center displacement but tunable barrier heights it is evident that the relaxation rates (depending exponentially on U_δ) change in a continuous but strong way under pressure. Consequently, a relaxation rate τ^{-1} corresponding to a particular measurement frequency shifts under pressure to lower and lower temperatures, often sweeping through regions of various predominant relaxation mechanisms (as indicated by the different $\tau^{-1}(T)$ dependencies [Figs. 10(c) and 13]). There is no indication that the temperature boundaries between regions, in which thermally activated reorientation, multiphonon- or one-phonon-assisted tunneling occurs, change appreciably under pressure.

This motional behavior of off-center ions (like Ag$^+$) under pressure, can in many respects be regarded as a "localized analog" to the motional behavior of small ions in *superionic conductors* (like Ag$^+$ in AgI). In both systems, the lattice framework supplies a large number of voids or sites (by far exceeding the number of Ag$^+$), among which the ions can move along a network of paths with low-potential barriers. While the motion of the Ag$^+$ ions through an *interconnected* network (in AgI) leads to superionic *conductivity*, the spatially restricted motion of the isolated Ag$^+$ in the multiwell off-center potential leads to an extremely high *local ionic polarizability*. The same small-size ions (Ag$^+$, Cu$^+$, Li$^+$, Na$^+$, F$^-$) give rise to off-center and superionic conduction behavior.

For both types of systems, the achievement of an optimum-ionic mobility depends critically on the size match between channel and migrating ion.[35] Too large misfits (small particles in very large channels) are *not* advantageous, resulting in large barriers and trapping of the ion in off-center states. Examples are our "deep off-center systems" (e.g., Cu$^+$ in potassium and rubidium halides) and on the other side Li$^+$ in β-alumina. A closer match (Cu$^+$ in NaBr and Na$^+$ in β-alumina) produces lower barriers and high-ionic mobility. Hydrostatic pressure supplies in both cases the "fine tuning" to influence these matching effects further, leading, e.g., to very different pressure effects on the conductivity of Li$^+$, Na$^+$, and K$^+$ ions in β-alumina.[36] (Li$^+$ in β-alumina becomes more mobile under pressure, similar to the off-center systems.)

Several superionic conductors show besides this conductive (equal to diffusive) ionic motion additionally dielectric effects (involving very small

TABLE III. Critical pressure (P_c) and lattice parameter change ($-\Delta a/a$) for the off- to on-center transition, observed optically (f) and dielectrically (δ).

System	P_c (kbar)	$-\Delta a/a$ (%)
NaBr:Cu^+	2.7 (f, δ)	0.38
RbCl:Ag^+	1.3 (f, δ)	0.23
RbBr:Ag^+	2.7 (f)	0.53
RbBr:Ag^+	3.6 (δ)	0.70

barrier heights), due to ionic motion in spatially restricted regions. These latter effects, observed, e.g., in Li_3N at low temperatures[37] and not fully understood, may have even closer similarities to our off-center defect model systems.

B. Transition from off- to on-center behavior

At a critical pressure P_c, characteristic for each system, the dipolar dielectric response and the uv oscillator strength drop in a very narrow pressure range, indicating an off- to on-center transition of the defect ion. In RbCl:Ag^+ and NaBr:Cu^+ this transformation appears within the experimental accuracy for each system at the *same* critical pressure P_c, when measured dielectrically and optically (Fig. 16 and Table III). Only in RbBr:Ag^+, a considerable discrepancy in the $\langle p \rangle(P)$ and $f(P)$ behavior is observed, for which no explanation is yet available.

As indicated in the Introduction, this off- to on-center transformation can be regarded as a localized analog to displacive phase transitions of ferroelectrics under pressure (Fig. 1). While, however, the latter are cooperative phenomena of a whole sublattice of displacement dipoles, the off- to on-center transition of the dilute (i.e., basically interaction-free) defect system is a property of the isolated defect ion and its lattice surrounding, produced solely by the changing lattice spacing.

Similar to the case of ferroelectrics, the question if this transition is of *first- or second-order character* (Fig. 1) is a very basic one. For the KCl:Li^+ system, a continuous shift of the tunneling splitting (consistent in infrared and in our dielectric measurements) and of the infrared resonance modes is observed.[30] These data could be fitted by Kahan *et al.* to a simple, one-dimensional square-well potential model, with a barrier height decreasing gradually under pressure. (This simplified double-well model naturally disregards the difference between the central and reorientational barrier.) There is no question from these data and model calculations, that a *second-order transition with gradually tuning potential parameter* is the appropriate one for KCl:Li^+.

For the Cu^+ and Ag^+ systems, however, the available experimental data and theoretical models are not that decisive, and allow to make in principle a case in two different directions.

1. Second-order transition

The observed gradual reduction of the central and rotational barriers U_f and U_6 (Fig. 17) extrapolate to zero at pressures close to the measured P_c values (indicated by arrows in Fig. 17). This is a very strong argument *for* a second-order-type off- to on-center transition, caused by continous tuning of the multiwell potential into a centrosymmetric one [Fig. 1(a)]. An argument *against* this interpretation appears to be the observed abrupt drop in the off-center displacement, which is in contrast to the prediction from Nagasaka's calculation.[16] This latter treatment, however, determines the off-center displacement *classically* from the distance between the potential well minima, which obviously tunes to zero in a gradual fashion. In an appropriate quantum-mechanical model, the off-center displacement is given by the wave-functions in the lowest states, which lie *above* the potential minima by the amount of the zero-point energy. The transition from off- to on-center behavior is expected, when the central barrier is tuned below this zero-point energy.[33] This transition, therefore, can appear still within the (very shallow) multiwell potential and in a much more abrupt way than the classical model predicts.

Another argument against a second-order picture may be seen in the contrast of the abrupt changes in the Cu^+ and Ag^+ systems, compared to the gradual tuning in KCl:Li^+. Both types of systems are characterized by *similar barrier heights U_f and U_6 and pressure tuning dU/dP* (Fig. 17) but very *different masses* of the mobile ion. For the light-mass Li^+ ion, these barriers produce already at $P = 0$ a sizable and directly measurable tunneling splitting, which tunes under pressure gradually to larger values (Fig. 15). For the heavy mass Ag^+ and Cu^+ ions, on the other hand, the tunneling splitting Δ at $P = 0$ is extremely small and not directly measurable. Its increase under pressure $\Delta(P)$, however, can be observed indirectly by the dramatic increase of the relaxation rate $\tau^{-1}(P)$ in the low-temperature range of one-phonon-assisted tunneling. For Cu^+ in NaBr, the relaxation rate is found to increase by two orders of magnitude between $P = 2.14$ and 2.50 kbar [Fig. 10(c)]. As this rate depends quadratically on Δ [Eq. (12)], $\Delta(P)$ must increase by about three orders of magnitude per kilobar in the range $P < P_c$. A similarly strong $\Delta(P)$ increase can be de-

duced from the observed low temperature $\tau^{-1}(P)$ dependence in RbBr:Ag^+ (Fig. 13). Close to P_c, at extremely small barriers, $\Delta(P)$ becomes sizable enough to be directly observable in the dielectric response: for NaBr:Cu^+ at $P = 2.5$ kbar [Fig. 10(a)] $\Delta \approx 12$ K, and for RbCl:Ag^+ at 1.2 kbar (Fig. 11) $\Delta \approx 7$ K. As for RbCl:Ag^+ at atmospheric pressure the tunneling splitting has been estimated (from paraelectric resonance experiments[34]) to be smaller than 0.01 K, we can deduce for this system too a $\Delta(P)$ increase of about three orders of magnitude per kilobar. Therefore the main difference between the light-mass (Li^+) and heavy-mass (Ag^+, Cu^+) systems appears to be the fact, that *a similar tuning of the potential $U(P)$ produces for* Ag^+ *and* Cu^+ *a much stronger* $\Delta(P)$ *variation* [starting at extremely small $\Delta(0)$ values], compared to the modest $\Delta(P)$ variation of the KCl:Li^+ system.

The tunneling splitting and its pressure tuning $\Delta(P)$ determines decisively the dipolar response around P_c, i.e., at small barrier heights. As in a quantum-mechanical model a state with dipole moment $\langle p \rangle$ must always be formed by a linear combination of gerade and ungerade tunneling eigenstates, Langevin-Debye polarization with $\epsilon_D \propto p^2/T$ behavior will occur only for $T > \Delta$, while for $T < \Delta$ ϵ_D will level off at a value $\epsilon_D \propto \langle p \rangle^2/\Delta$. The KCl:$Li^+$ system shows the gradual evolution of this dielectric response due to $\Delta(P)$ tuning by the shift of the $\epsilon_D \propto T^{-1}$ range to high temperatures and by the decrease of the low-temperature response $\epsilon_D \propto \Delta^{-1}$ (Fig. 14). These effects make an experimental determination of $\langle p \rangle$ from ϵ_D data (on top of the large background ϵ_β) towards high pressure more and more uncertain and finally impossible (Fig. 15).

For the Ag^+ and Cu^+ systems these effects happen in a very narrow pressure range due to their much stronger $\Delta(P)$ variation. While low-temperature saturation effects $\epsilon_D \propto \Delta^{-1}$ appear abruptly at a particular pressure, the next higher P value may already increase Δ enough such that the $\epsilon_D \propto \Delta^{-1}$ and $\epsilon_D \propto T^{-1}$ response disappears in the background response of the host material. This blows up vastly the error bar for $\langle p \rangle$ and prevents an exact determination of the $\langle p \rangle(P)$ variation.

In summary: Within these error bars and the expected differences resulting from the different $\Delta(P)$ variation, the behavior of both the Li^+ and the Ag^+ (Cu^+) systems are well compatible. All results can be at least qualitatively accounted for in a picture of a gradual second-order potential tuning under lattice compression.

2. *First-order transition*

An alternative explanation has become attractive by the work of Kleppman,[38,39] who calculated microscopic models for Ag^+ in RbCl and RbBr, extending the earlier treatments[5,6] in two directions: (i) He included a sizable *quadrupolar deformability* (QD) for the Ag^+ ion (which is based on the presence of the low-lying $d \rightarrow s$ electronic transitions, studied in this work). (ii) He allowed *noncubic relaxation* of the nearest-neighbor anions around the defect.

For a particular ("cigar-shaped") deformation of the Ag^+ ion and E_g lattice distortion around the defect, Kleppmann obtains for the first time a multiwell potential with *absolute minima in the* $\langle 110 \rangle$ *directions* [earlier treatments[5,6] without (i) and (ii) always predicted $\langle 111 \rangle$ minima]. For a different ("disk-shaped") deformation of the Ag^+ ion and a different E_g distortion, Kleppmann obtains an alternative potential for the Ag^+ ion with a minimum in the centrosymmetric position. As the latter is computed to lie in energy by $\Delta U = 13$ K *above* the off-center minima, the $\langle 110 \rangle$ off-center states should be the stable configuration as observed. Under an assumed lattice compression, ΔU is found to decrease steadily, and Kleppmann calculates for reasonable choice of the QD parameter and the Ag^+ ion radius[38] that both configurations should become equal in energy ($\Delta U = 0$) at a lattice spacing corresponding closely to our measured P_c values. At this critical pressure one would therefore expect an abrupt first-order-type transition from the off-center configuration (with large $\langle p \rangle$) into the on-center configuration with $\langle p \rangle = 0$.

The abrupt way in which this transition is observed for the Cu^+ and Ag^+ defects is certainly in agreement with this picture. A rather strong counterargument, however, is the fact, that the calculations predict very little reduction in the barrier heights for $P < P_c$. This is in contrast to our observed very strong reduction of U_δ and U_f which tend to zero at P_c (Fig. 17). *This latter argument favors from the experimental side strongly the second-order transition picture.*

Direct experimental tests differentiating between the two pictures could be achieved by spectroscopy on the low-lying motional states of Ag^+ and Cu^+ under pressure. If the *second-order* picture is right, dramatic increases of $\Delta(P)$ should occur (about three orders of magnitude per kilobar!) which could be measured by paraelectric resonance or far-infrared spectroscopy. The low-lying-resonance modes ω_R, on the other hand, should soften under pressure-tuning of the potential, similar to the *soft-mode behavior* in second-order phase transitions [see Fig. 1(a)]. If Kleppmann's first-order-transition picture is right an abrupt change of all low-lying modes should occur at P_c [see Fig. 1(c)]. Experiments with Raman

scattering under pressure, directed at this question and other aspects of these model defects in tunable potentials, are under preparation.

ACKNOWLEDGMENTS

We are indebted to Professor B. G. Dick, Professor H. Monkhorst, and Professor R. Orbach for helpful and stimulating discussions, and to Dr. W. G. Kleppmann for permission to reproduce a figure from his Ph.D. thesis. This work was supported by NSF under Grant No. DMR74-13870 and No. DMR77-12675.

APPENDIX

It should be pointed out, that in principle an alternative interpretation of the observed relaxation changes under pressure can be considered too. The relaxation rate for phonon-assisted tunneling depends not only on the potential barrier, but additionally on the noncubic lattice distortion produced by the elastic and electric dipole moment of the defect. This "dressing" or polaron aspect of the defect leads to a renormalization of the original "bare" tunneling matrix element Δ_0 to yield an effective value.

$$\Delta_{eff} = \Delta_0 \exp(-W_0) . \tag{15}$$

W_0 is a kind of Debye-Waller factor from the lattice coupling, which is proportional to the square of the electric and elastic dipole moment.[8,9] Therefore the observed increase of relaxation rates under pressure can in principle be explained by a reduction of this dressing parameter W_0 (rather than by an increase of Δ_0 due to barrier reduction).

This model can in principle also explain the observed relaxation changes in the high-temperature exponential range [Eq. (11)]. An extension of the tunneling model leads in the high-temperature limit to an Arrhenius-like expression,[40] with the preexponential factor proportional to the square of the bare-tunneling-matrix element Δ_0^2, and an "activation energy" determined by the defect lattice coupling W_0 (and *not* related to the static-barrier height). Though such a behavior should normally occur in a range above the half Debye temperature, low-lying resonance-phonon modes could bring this effect down to much lower temperatures.[40] Therefore the observed reduction of the activation energy U_δ (Fig. 17) could in principle originate from a pressure tuning of the lattice coupling $W_0(P)$.

Is such an alternative interpretation likely to be true? We do not believe so for the following reasons: our experiments show clearly that the electric dipole remains nearly unchanged for $P<P_c$, so that a $W_0(P)$ tuning can definitely *not* arise from the T_{1u} dressing from *electric* polarization, but had to arise from a tuning of the *elastic* dressing $\beta(E_g)$ and $\beta(T_{2g})$. It is hard to understand why a defect with constant electric dipole (equal to the off-center displacement) should exhibit such a drastic reduction of the elastic dipole under pressure. It is equally hard to understand why an off- to on-center transition should take place, when the lattice coupling W_0 is tuned to zero. Moreover, the observed decrease of the pre-exponential factor under pressure would mean in this tunneling model a decrease of the bare tunneling model Δ_0, i.e., an *increase of the potential barriers.* Such a behavior would be in contrast to all model calculations and to the KCl:Li^+ spectroscopic results.

For these reasons we have assumed throughout this work, that the lattice coupling W_0 remains rather constant under pressure and that the observed drastic relaxation changes arise, at least mostly, from tuning of the potential barriers $U_\delta(P)$, i.e., $\Delta_0(P)$. A crucial experiment to decide this question would be a measurement of the elastic dipole components $\beta(E_g)$ and $\beta(T_{2g})$ under pressure. If they remain (similar as $\langle p \rangle$) constant for $P<P_c$ it would be proven that the observed activation energy U_δ is not related to the lattice coupling W_0 but to the static potential, and that the pressure tunes potential barriers and Δ_0 rather than W_0.

---

*Present address: Hindenburgring 31, 7900 Ulm, West Germany.

[1] G. Shirane, H. Danner, and R. Pepinsky, Phys. Rev. 105, 856 (1957).

[2] For a review of "off-Center Substitutional Ions," see R. Smoluchowski, in *Proceedings of Colloque Ampere* (North-Holland, Amsterdam, 1969), Vol. XV; for more recent references, see M. F. Deigen and M. D. Glinchuk, Sov. Phys. Usp. 17, 691 (1975).

[3] A. S. Nowick and W. R. Heller, Adv. Phys. 12, 251 (1963).

[4] G. A. Samara, in *Advances in High Pressure Research*, edited by R. S. Bradley (Academic, New York, 1969), Vol. 3, p. 155.

[5] W. D. Wilson, R. D. Hatcher, R. Smoluchowski, and G. J. Dienes, Phys. Rev. 184, 844 (1969).

[6] R. J. Quigley and T. P. Das, Phys. Rev. 177, 1340 (1969).

[7]Some preliminary results have been presented at the International Color Center Conference, Sendai, Japan 1974 (unpublished), and at the 1975 Ferroelectricity Meeting in Puerto Rico as seen in U. Holland and F. Luty, Ferroelectrics 17, 377 (1977).
[8]H. B. Shore and L. M. Sander, Phys. Rev. B 12, 1546 (1975).
[9]B. G. Dick and D. Strauch, Phys. Rev. B 2, 2200 (1970).
[10]For more details on the apparatus, experimental techniques and results not included here, see U. Holland, Ph.D. thesis (University Utah, Salt Lake City, 1976) (unpublished).
[11]J. S. Dugdale, Nuovo Cimento Suppl. 9, 27 (1958).
[12]K. Knop, dissertation (Eidgenössische Technische Hochschule, Zürich, 1974) (unpublished).
[13]J. T. Lewis, A. Lehoczky, and C. V. Briscoe, Phys. Rev. 161, 877 (1967); M. H. Norwood and C. V. Briscoe, *ibid.* 112, 45 (1958); R. N. Claytor and B. J. Marshall, *ibid.* 120, 332 (1960).
[14]P. W. Bridgman, *Physics of High Pressures* (Macmillan, New York, 1931), p. 163.
[15]K. Fussgaenger, Phys. Status Solidi 34, 157 (1969); 36, 645 (1969).
[16]S. Nagasaka, Japanese translated into English by Shigeru Yamada (Department of Computer Science, Univ. Utah, Salt Lake City, 1977) (unpublished). (All equations in Sec. III are from this paper.) Similar calculations were presented by S. Nagasaka, in International Conference on Color Centers in Ionic Crystals, Sendai, Japan, 1974 (unpublished).
[17]M. D. Glinchuk, M. F. Deigen, and A. A. Karmazin, Sov. Phys. Solid State 15, 1365 (1974).
[18]R. V. Jimenez and F. Luty, Phys. Rev. B 12, 1531 (1975).
[19]S. Kapphan and F. Luty, Phys. Rev. B 6, 1537 (1972).
[20]S. Emura, M. S. thesis (Laboratory of Applied Physics, Kyushu Institute of Technology, Katsksyushu-Shi, Japan 804, 1974) (unpublished).
[21]A. I. Laisaar and Ya. Ya. Kirs, Bull. Acad. Sci. USSR Phys. Ser. 33, 917 (1969); C. S. Kelley, Phys. Rev. B 12, 594 (1975); D. I. Klick, K. W. Bieg, and H. G. Drickamer, Phys. Rev. B 16, 4599 (1977).
[22]M. Gomez, S. P. Bowen, and J. A. Krumhansl, Phys. Rev. 153, 1009 (1967).
[23]S. A. Letzring, M. S. thesis (Cornell Univ., Ithaca, N. Y., 1969) (unpublished).
[24]For a good introduction, see A. S. Nowick and B. S. Berry, *Anelastic Relaxation in Crystalline Solids* (Academic, New York, 1972).
[25]For a reveiw on orientation behavior, see F. Luty, J. Phys. C (Paris), 9, 49 (1973).
[26]R. P. Lowndes and D. H. Martin, Proc. R. Soc. A 308, 473 (1969).
[27]E. E. Havinga and A. J. Bosman, Phys. Rev. 140, A292 (1965).
[28]R. Sittig, Phys. Status Solidi 34, K189 (1969).
[29]M. S. Li, M. de Souza, and F. Luty, Phys. Rev. B 7, 4677 (1973).
[30]A. M. Kahan, M. Patterson, and A. J. Sievers, Phys. Rev. B 14, 5422 (1976).
[31]R. A. Herendeen and R. H. Silsbee, Phys. Rev. 188, 645 (1969).
[32]J. Wahl and F. Luty, Ferroelectrics 17, 371 (1977).
[33]A. S. Barker and A. J. Sievers, Rev. Mod. Phys. 47, Suppl. 2 (1975).
[34]F. Bridges, Crit. Rev. Solid State Sci. 5, 1 (1975).
[35]W. H. Flygare and R. A. Huggins, J. Phys. Chem. Solids 34, 1199 (1973).
[36]R. H. Radzilowski and J. T. Kummer, J. Electrochem. Soc. 118, 714 (1971).
[37]J. Wahl and U. Holland, Solid State Commun. 27, 237 (1978).
[38]W. G. Kleppmann, J. Phys. C 9, 2285 (1976).
[39]W. G. Kleppman, Ph.D. thesis (Univ. of Oxford, Oxford, England, 1977) (unpublished).
[40]B. G. Dick, Phys. Rev. B 16, 3359 (1977).